Euro-Mediterranean Journal for Environmental Integration (2018) 3:39
https://doi.org/10.1007/s41207-018-0080-y

ORIGINAL PAPER

Kinetics of uranium and iron dissolution by sulfuric acid from Abu Zeneima ferruginous siltstone, Southwestern Sinai, Egypt

Bahig M. Atia[1] · **Mohamed A. Gado**[1] · **Mohamed F. Cheira**[1]

Received: 16 May 2018 / Accepted: 30 August 2018 / Published online: 12 September 2018

Abstract

This study deals with kinetic studies of uranium and iron dissolution using sulfuric acid from Abu Zeneima ferruginous siltstone, Southwestern Sinai, Egypt. The importance of this study stems from the fact there is a difference in the dissolution rate and activation energy which allows the separation of the two elements from each other through the dissolution units without entering the extraction units. The influence of H_2SO_4 concentration, temperature, stirring speed, particle diameter and solid to liquid phase ratio was examined. The dissolution rate was greatly influenced by the studied dissolution factors. Kinetic data analysis showed that the dissolution mechanism follows the shrinking core model with chemical reaction as a rate determining step with an activation energy (E_a) of 31.59 kJ/mol for uranium and (E_a) of 26.02 kJ/mol for iron. The dissolution study showed that 0.8 M H_2SO_4 can dissolute approximately 81.92% of uranium and 96.94% of iron at 90 °C with 400 rpm stirring, 0.074 mm particle diameter and 5/50 g/ml (S/L) phase ratio.

Keywords Uranium dissolution · Iron dissolution · Uranium dissolution kinetics · Shrinking core model

Introduction

Uranium is one of the most important heavy metals because of its strategic significance in the energy field. The leaching of uranium is a term to describe the process of extracting uranium from its ore which considered as an essential step in the uranium processing. Uranium leaching is carried out via conventional or non-conventional techniques depending on the type of uranium mineral, uranium ore grade, reagents availability, economics of the process and environmental impacts (Cheira et al. 2014; Azimi and Azari 2017; Gado 2018).

Uranium could actually be leached from its ore materials by either acid or alkaline leaching. The choice of the best reagent depends on various technical and economic aspects, namely type of uranium mineral, gangues, availability and reagents costs, oxidant requirements and construction materials of the equipment. In uranium leaching, several variables must be assessed to determine the optimum leaching conditions such as grain size, slurry density, degree of agitation composition of leach liquor, reagent conc., oxidation potential, temperature, pressure and leaching time (kinetics and leaching mechanism) (International Atomic Energy Agency 1990).

The kinetics and practical facts of the uranium leaching, HSS system (H_2O_2–Na_2SO_4–H_2SO_4) were applied on the typical New Mexico ore material at temperature ranged between 30 and 80 °C and constant pH 4.6. The effect of Na_2SO_4 and H_2O_2 concentration, pH, temperature and Fe^{2+} addition on the rate of uranium extraction was determined (Eligwe et al. 1982; Yildiz et al. 2017a; Sen et al. 2017a, b, c, d). Studying the oxidation of uranium species coming from some Romanian uranium ores in the presence of some oxidizing agents such as $KMnO_4$ or H_2O_2 with H_2SO_4 was carried out. The leachability of some natural and man-made radionuclide from soils and sediments was subject to attack by various acid mixtures such as 6 M HCl, 8 M HNO_3 and/or 8 M aqua regia at a temperature range 20–75 °C for the time intervals from 2 to 24 h. The data indicated that the use of H_2SO_4 resulted in 25% overall increase in the minerals dissolution (Benedik et al. 1999).

Recently, (Smirov et al. 2009) the kinetic features of underground uranium leaching from Russian ores of hydrogenous uranium deposits were explained. A dilute aqueous acidic ferric nitrate solution (0.002 M) was used to extract

✉ Bahig M. Atia
dr_bahig.atia@yahoo.com

[1] Nuclear Materials Authority, P.O. Box 530, El Maadi, Cairo, Egypt

97% of uranium (IV) from ores occurring in the Elliot Lake area of Canada at optimum leaching conditions which are 0.1 g/ml S/L phase ratio, at 75 °C for 24 h.

A comparative batch and counter-current acid leaching were conducted on low-grade Quirke Mine and high-grade complex Midwest Lake, Canada uranium ores with various oxidants. The leaching results indicate that uranium extraction is least affected by the kind of oxidant and type of leaching but counter-current leaching generally provides higher uranium extraction (Haque and Laliberte 1987). The leaching of uranium from raw phosphorite was studied using sodium carbonate leachate at high selective temperature (Ketzinel et al. 1984). An oxidative leaching of uranium from SIMFUEL using Na_2CO_3–H_2O_2 leachate was also proposed by Chung et al. (2010).

Several kinetic studies of UO_2^{2+} dissolution using different leaching agents with different oxidants were carried out (Amme et al. 2007; Sharma et al. 1996; Goff et al. 2008; Peper et al. 2004; Lee et al. 2009). The oxidation of Fe^{2+} in uranium leaching solutions with a gaseous system mixture of SO_2 and air was studied (Umanskii and Klyushnikov 2011). The kinetic of leaching process of uranium from EL-Missikat shear zone eastern desert and El-Erediya rock, Sella rock (Khawassek et al. 2016a, b) and El-Hammamat sediment in Egypt were applied by sulfuric acid solution.

The mineral monazite is a naturally occurring rare earth phosphate in which uranium and thorium commonly substitute for the REES in the cation sub-lattice. A modified alkaline dissolution of Egyptian monazite was applied and it was found that uranium could be selectively leached by a mixture of sodium carbonate, sodium hydroxide and hydrogen peroxide leaving thorium and rare earth elements as an insoluble hydrous oxide (El-Nadi et al. 2005). The leaching of uranium from monazite specimens with carbonate–bicarbonate leachate was explained (Eyal and Olander 1990a, b, c).

In recent times, the determination of U(VI) and U(IV) in phosphate ores (El-Sebayia, Qatrani and Abu Tatur) through HCl selective leaching was suggested by Fouad (2010). The uranium recovery from a uranium-bearing phosphatic sandstone (phosphate reserves present in Qatrany area, south west of Cairo with a uranium assay of 0.048% U) was proposed using a heap leaching technique using $Fe_2(SO_4)_3$/H_2SO_4 leachate (Shakir et al. 1992a, b).

Moreover, the bioleaching is an interesting branch of hydrometallurgy used for metal extraction from their ores using microorganisms. The microbial technique offers an economic alternative for the mining industry at a time the high-grade mineral resources are being depleted (Devasia and Natarajan 2004). The bioleaching treatment of Abu Zeneima uraniferous Gibbsite ore for uranium recovery was applied (Ibrahim and El-Sheikh 2011).

Furthermore, the dissolution of alkali metal urinates in carbonate melts under the influence of CO_2 and O_2 partial pressure was performed (Volkovich et al. 2000). Billard et al. (2007) studied the dissolution of UO_2 and UO_3 in the ionic liquid, 1-methyl-3-butyl imidazolium bis-triflimide (BumimTf_2N) with the help of small amounts of HNO_3 leading to the formation of $UO_2(NO_3)_3^-$. The imidazolium-based Fe-containing ionic liquids (ILS) were directly dissolved UO_2^{2+} in the presence of their corresponding imidazolium chlorides without additional oxidants (Yao and Chu 2013). A comparative study on the dissolution rate of sintered (Th–U)O_2 pellets in nitric acid by microwave and conventional heating was also reported (Singh et al. 2011). The basic features of the leachability of depleted uranium (DU) projectiles in soil were surveyed (Schimmack et al. 2005; Pulhani et al. 2007).

This study deals with the current state of uranium leaching from Abu Zeneima ferruginous siltstone, Southwestern Sinai, Egypt, using H_2SO_4 acid. The kinetic aspects of uranium leaching and the examination of the effects of the main system variables are investigated on the leaching rate, as well as the apparent activation energy for uranium (VI) and iron (III).

Experimental

Materials and methods

All reagents used in the experiments were prepared from analytical grade chemicals (Fluka, POCH S.A. Poland and Scharlau Chemie S.A. Spain).

Abu Zeneima ferruginous siltstone sample was obtained from Abu Zeneima area, Southwestern Sinai, Egypt. The rock was crushed, grinded and sieved with American Society for Testing and Materials (ASTM) standard sieves into four size fraction; 0.297, 0.149, 0.105 and 0.074 mm mesh size.

The chemical composition of Abu Zeneima ferruginous siltstone sample has been determined as major oxides by colorimetry technique and the traces by ICP-OES technique (Prodigy High Dispersion ICP, TExxLEDYNE-Leeman Labs USA). The quantitative analysis of uranium was carried out by a single beam spectrophotometer, Meterch Inc (SP-8001) using Arsenazo III indicator (Janberty et al. 2013) and confirmed by an oxidometric titration against ammonium metavanadate using *N*-phenyl anthranilic acid indicator by computerized titrator, SCOTT instrument, GmbH, Germany (Mathew et al. 2009). The mineralogical composition of the shale sample was examined using XRD, PHILIPS PW 3710/31 diffractometer, Scintillation counter, Cu-target tube and Ni filter at 40 kV and 30 mA. EDAX with scanning electron microscope (SEM) pictures is used to indicate the

mineralogical state of the Abu Zeneima ferruginous siltstone ore and its solid residue after dissolution.

Experimental dissolution procedures

Experiments were carried out by agitation leaching using a covered 500-ml Pyrex flask and mechanically stirred with a magnetic stirring bar at 0–400 rpm. Typically and for each run, 50 ml of H_2SO_4 solution of a definite molarity was charged into the glass reactor and heated to the required temperatures. Thereafter, 5 g of the shale sample was added and the contents were well agitated. The concentration of H_2SO_4 which gave the maximum dissolution of uranium and iron was subsequently used for the optimization of the other dissolution parameters. The fraction of uranium and iron dissolved (X) was calculated from the initial difference in weight of the amounts dissolved and undissolved at various time intervals up to 60 min (Ayanda and Adekola 2012).

Table 1 Chemical composition of Abu Zeneima ferruginous siltstone ore sample and its post-dissolution solid residue

Oxide (%)	Abu Zeneima sample	Post-dissolution solid residue	Leachability, %	Trace elements, mg/kg	Abu Zeneima sample	Post-dissolution solid residue	Leachability, %
SiO_2	50.09	46.6	6.96 ± 0.382	U	498	90	81.92 ± 0.0.644
Al_2O_3	9.42	5.96	36.7 ± 0.191	Ga	275	104	62.18 ± 1.332
Fe_2O_3	18.03	0.55	96.94 ± 0.988	Zr	3288	1087	66.94 ± 0.687
CaO	3.52	1.2	65.9 ± 1.271	Pb	54	20	62.96 ± 2.788
MgO	2.15	1.54	28.37 ± 2.013	Cr	316	193	38.92 ± 0.937
P_2O_5	3.83	2.94	23.23 ± 1.621	Sr	26	9	65.38 ± 2.44
Na_2O	2.74	0.57	79.19 ± 2.77	Cu	547	186	65.99 ± 0.856
K_2O	1.89	0.78	58.73 ± 0.723	Y	103	31	69.9 ± 1.882
TiO_2	0.76	0.61	19.73 ± 2.223	Nb	108	35	67.59 ± 0.523

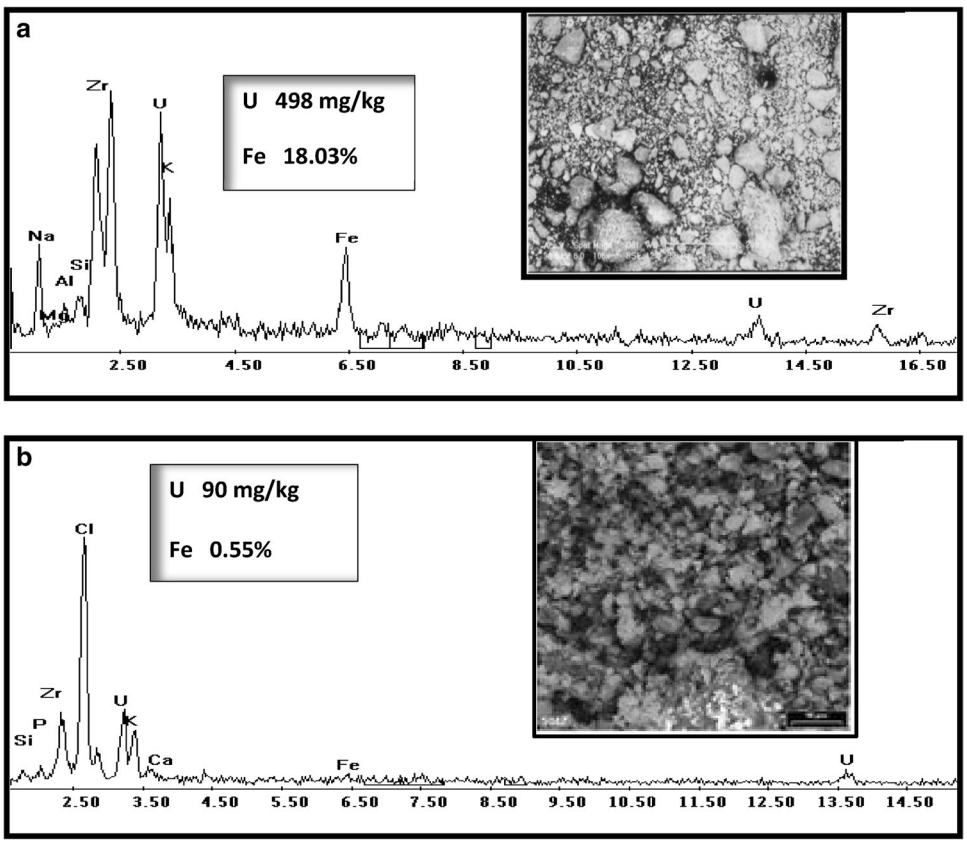

Fig. 1 SEM images and EDAX pattern of **a** Abu Zeneima ferruginous siltstone ore, **b** post-dissolution solid residue

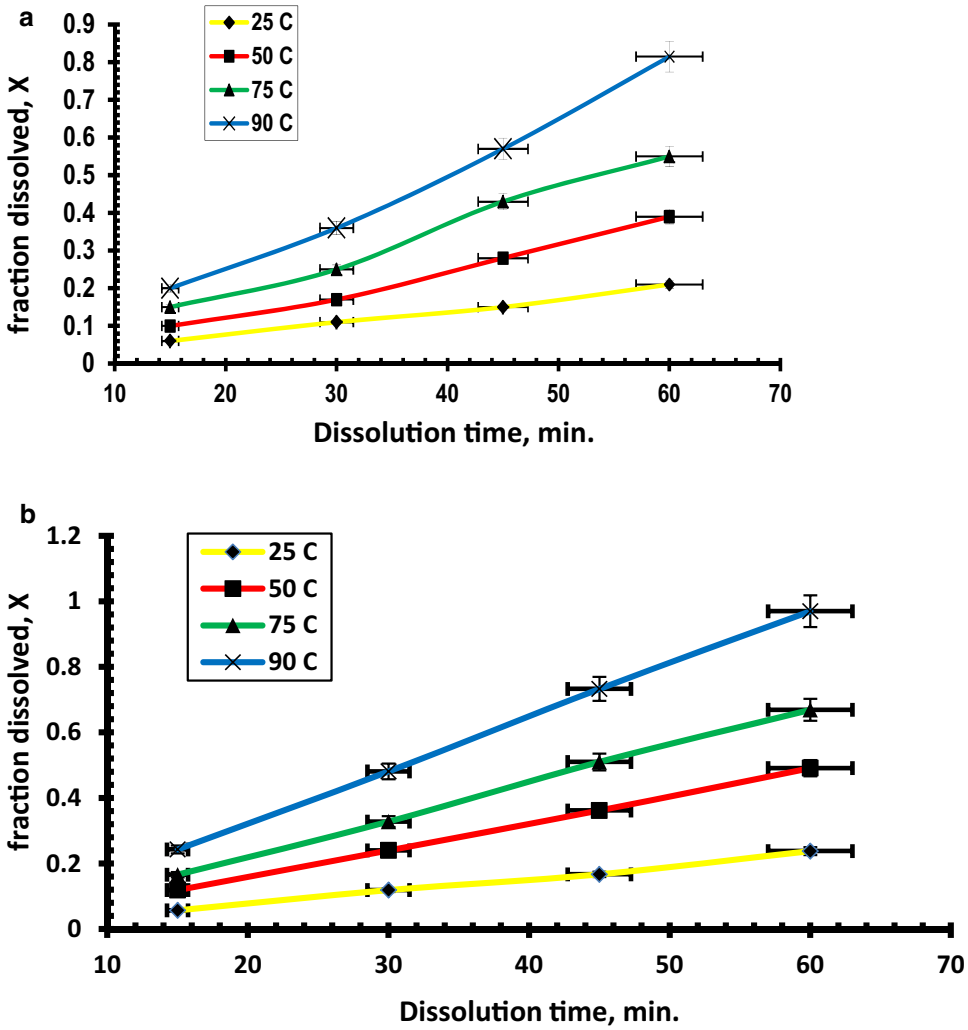

Fig. 2 Effect of temperature on fraction dissolved of **a** uranium **b** iron conditions: 5 g ore, 50 ml of 0.8 M H_2SO_4, 0.074 mm size fraction, 400 rpm

After oven drying at 50 °C, The post-dissolution residual was scanned and analyzed by both EDAX and ICP-OES techniques.

Results and discussion

Characterization of Abu Zeneima ferruginous siltstone

The chemical composition of Abu Zeneima ferruginous siltstone ore and its post-dissolution solid residue were analyzed as major oxides and trace elements by ICP-OES (Table 1) and EDAX, SEM images (Fig. 1a, b). From the obtained data, it is clear that the concentration of Fe_2O_3 decreases from 18.03 to 0.55% (about 96.94% leachability) and uranium decreases from 498 to 90 mg/kg (about 81.92% leachability) using H_2SO_4 as leaching agent. The measurements were calculated as triplicates with relative standard deviation.

The EDAX pattern of the ore reveals high uranium and iron concentrations before dissolution, but after dissolution low concentration was found. Moreover, the micro-structure of the ore and its post-dissolution solid residue were determined by scanning electron microscope (SEM) which reveals a clear difference in surface morphology with coarse grains before dissolution (Fig. 1a), while a smooth grains and fine surface after dissolution (Fig. 1b) due to penetration effect of H_2SO_4 leaching agent.

On the other hand, the X-ray diffraction data reveal that the ore is dominated by Quartz (SiO_2), Hematite (Fe_2O_3), Kaolinite ($Al_2Si_2O_5(OH)_4$), Gypsum ($CaSO_4.2H_2O$) and Dolomite ($CaMg(CO_3)_2$) minerals and there is no a definite uranium mineralization. Uranium was suggested to exist as a deposit altered and replaced by other elements. After dissolution with H_2SO_4, uranium almost vanished from the undissolved residue under optimized dissolution conditions. Also, the concentration of some trace elements in the dissolute ferruginous siltstone increased by the penetration action of H_2SO_4. Furthermore, hematite mineralization is responsible

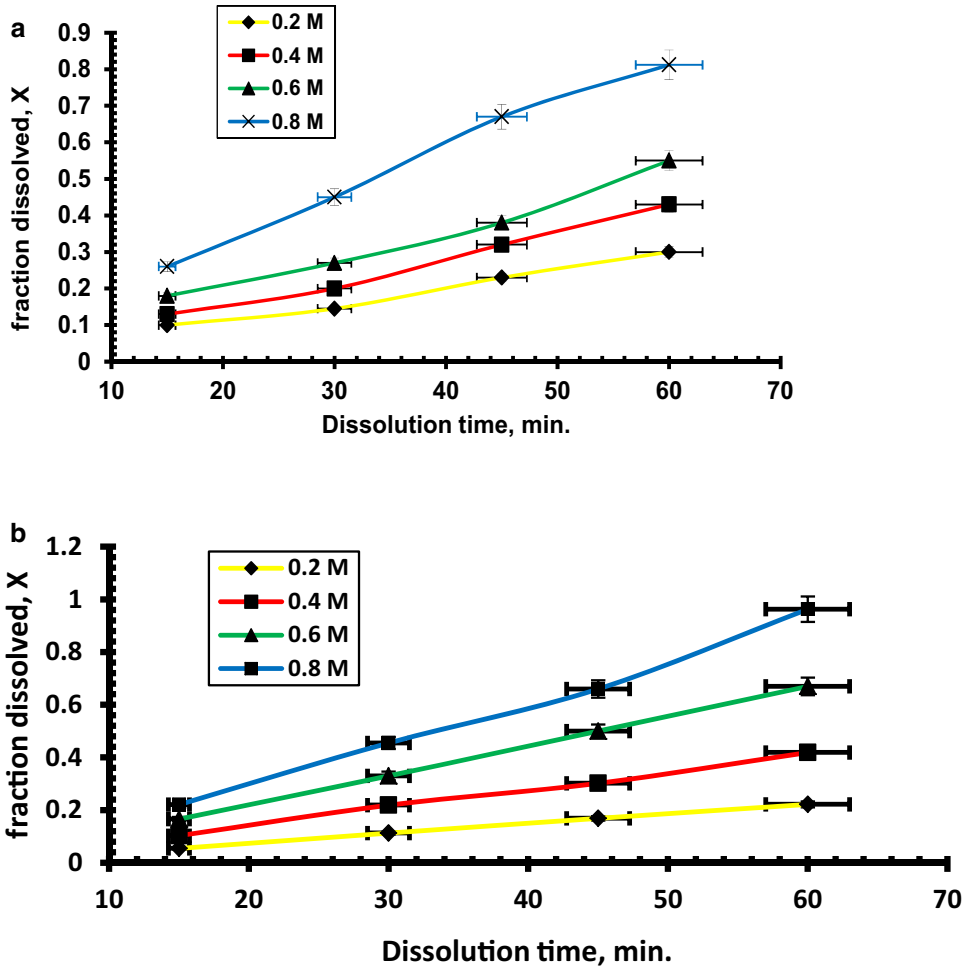

Fig. 3 Effect of H_2SO_4 concentration on fraction dissolved of **a** uranium **b** iron conditions: 5 g ore, 90 °C, 0.074 mm size fraction, 400 rpm

for the presence of iron in the ore which easily dissolved by sulfuric acid.

Uranium and iron dissolution studies

Temperature, H_2SO_4 concentration, particle size, stirring speed and solid to liquid phase ratio (*S*/*L*) are influential parameters affecting the dissolution of uranium and iron dissolution.

Effect of dissolution temperature

Temperature is a significant parameter especially in studying dissolution kinetics of uranium and iron from Abu Zeneima ferruginous siltstone ore. The fraction dissolved of uranium and iron was studied against dissolution time ranged between 15 and 60 min at different temperatures ranged between 25 and 90 °C. From Fig. 2a, b, it was observed that the fraction dissolved (*X*) of both uranium and iron increased with increasing both dissolution time and temperature. At 90 °C about 81.92% of uranium and 96.94% of iron were dissolved through 60 min. Hence, 60 min and 90 °C were used as optimum parameters for uranium and iron dissolution.

Effect of H_2SO_4 concentration

Sulfuric acid was chosen for special considerations of economic feasibility calculations, since it is cheap and available, but it has since proved to be non-selective as it dissolves uranium, iron and many impurities. Therefore, attention will then be given to studying the use of selective leaching agent or designing of extraction units to separate the two elements from each other.

The effect of H_2SO_4 concentration on uranium and iron dissolution rate from Abu Zeneima ore is explored in concentrations ranged between 0.2 and 0.8 M. In this study, other parameters were kept constant. From Fig. 3a, b, it was concluded that increasing H_2SO_4 concentration enhancing the uranium and iron fraction dissolves (*X*) attaining 0.8192 and 0.9694, respectively. Therefore, 0.8 M H_2SO_4 was chosen for optimum dissolution kinetics.

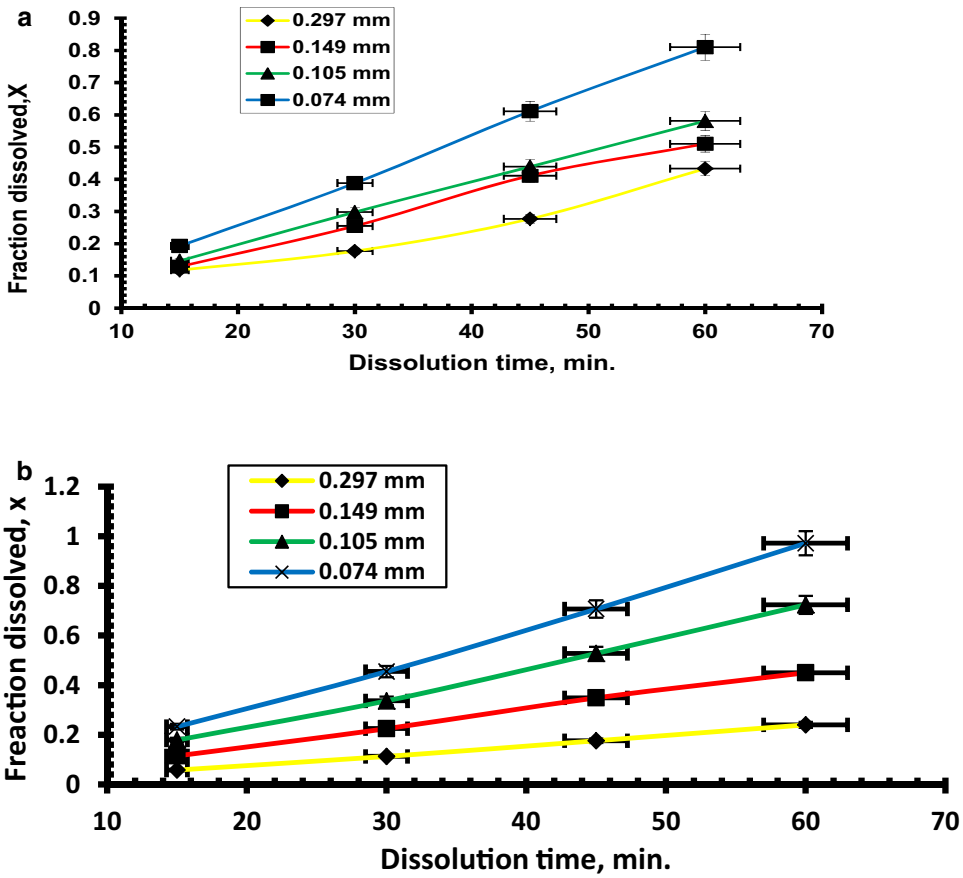

Fig. 4 Effect of particle diameter on fraction dissolved of **a** uranium **b** iron conditions: 5 g ore, 50 ml of 0.8 M H_2SO_4, 90 °C, 400 rpm

Effect of particle diameter

Particle diameter is an important factor which affects uranium–iron dissolution kinetics. Different particle diameter was examined in the range between 0.297, 0.149, 0.105 and 0.074 mm. The dissolution experiments were performed while other factors were kept constant. From Fig. 4a, b, it was found that the fraction dissolved (*X*) for both uranium and iron increased with decreasing the particle diameter due to the high surface area exposed to H_2SO_4 attack. Hence, 0.074 mm particle diameter was, therefore, chosen for further dissolution kinetics giving efficiency of 81.92% and 96.96% for uranium and iron, respectively.

Effect of solid to liquid phase ratio (*S*/*L*)

The effect of solid to liquid phase ratio (*S*/*L*) on the dissolution kinetics of uranium–iron was studied using ratios of 5/50, 6/50, 7/50 and 8/50 g/ml at constant optimized factors. As shown in Fig. 5a, b, it was found that increasing *S*/*L* ratio leads to decrease in uranium–iron dissolution rate as there is no enough H_2SO_4 concentration to complete the dissolution process. Hence 5/50 g/ml ratio was selected as optimum factor which gives the best uranium–iron dissolution rate.

Effect of stirring speed

The effect of stirring speed on uranium–iron dissolution kinetics using 0.8 M H_2SO_4 was studied at stirring speeds ranged between 100 and 400 rpm. Particle size of 0.074 mm, *S*/*L* ratio of 5/50 g/ml, and temperature at 90 °C were kept constant. According to the experimental data shown in Fig. 6a, b, it was observed that uranium–iron dissolution rate increases with increasing stirring speed. Hence, 400 rpm was chosen to give the best uranium and iron fractions dissolved.

Dissolution kinetic analysis

In a fluid–solid reaction system, the reaction rate is generally controlled by one of the following steps: diffusion through the fluid film, diffusion through the ash (or solid product) layer on the particle surface or the chemical reaction at the surface of the core of reacted particles. There are three controlling models for the rate of reaction: chemical reaction at the particle surface, diffusion through the product layer and a combination of both. The rate of the process is controlled by the slowest of these sequential steps (Karatepo et al. 2016; Yildiz et al. 2017b).

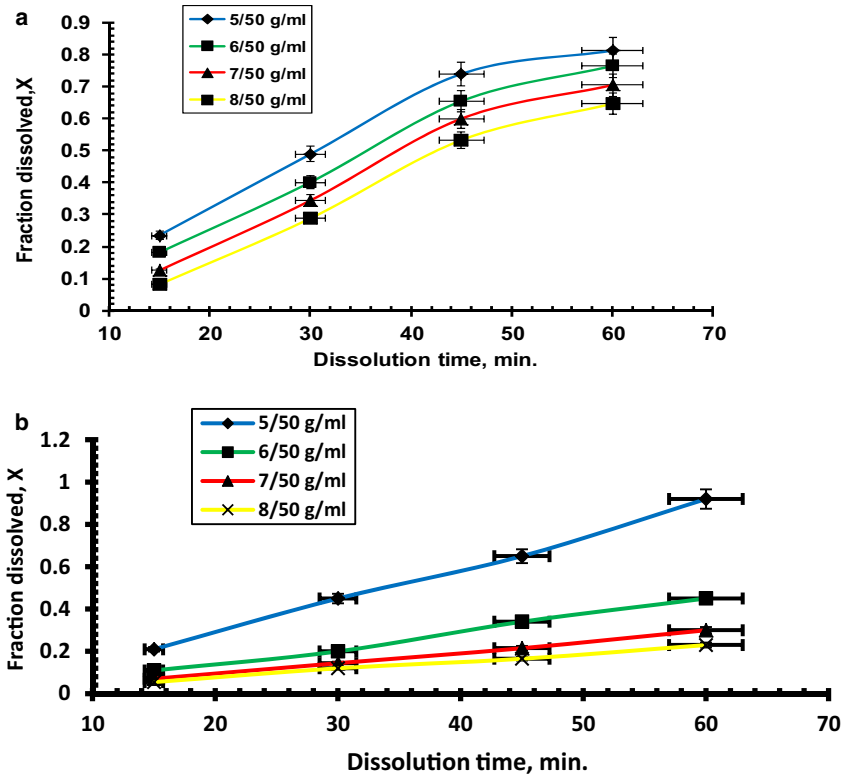

Fig. 5 Effect of *S*/*L* ratio on fraction dissolved of **a** uranium **b** iron conditions: 0.074 mm size fraction, 0.8 M H_2SO_4, 90 °C, 400 rpm

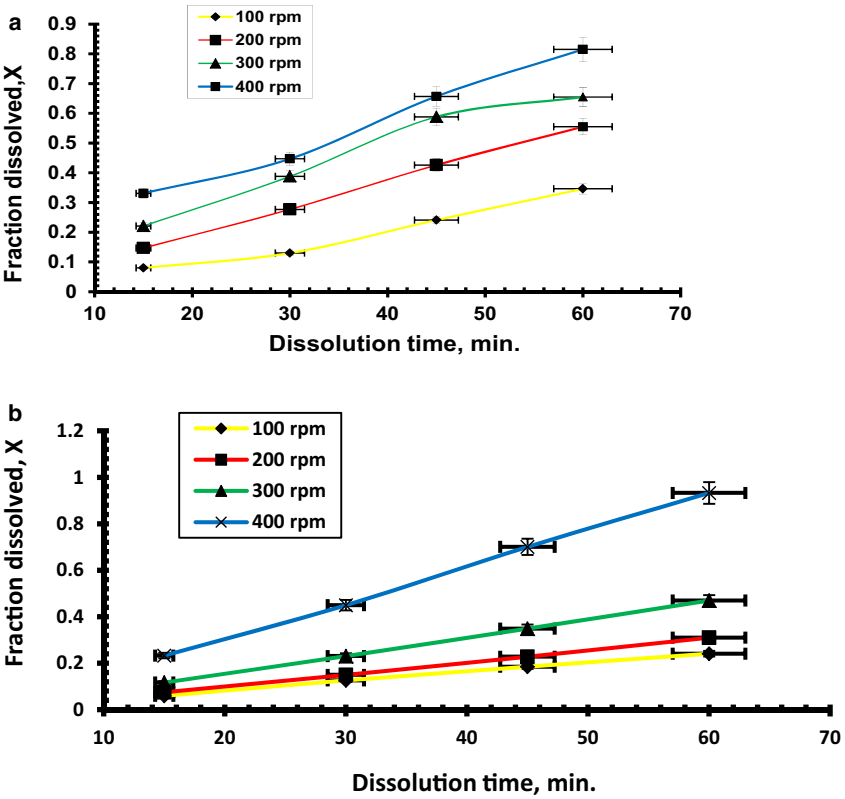

Fig. 6 Effect of stirring speed on fraction dissolved of **a** uranium **b** iron conditions: 0.074 mm size fraction, 0.8 M H_2SO_4, 90 °C, 5 g ore, 50 ml of 0.8 M H_2SO_4

The most important model suggested for derivation of the expression of the fluid–solid reaction is the shrinking core model (SCM) which is thought that the reaction takes place in the outer surface of the solid and this surface shrinks towards the center of the solid as the reaction proceeds leaving behind an inert solid layer, called ash layer, around the unreacted shrinking core (Wei et al. 2010; Dasdelen et al. 2017; Yildiz et al. 2016; Erken et al. 2015, 2016; Aday et al. 2016).

Considering that, a solid particle M is immersed and reacts with a fluid N as the following equation:

$$N\,(\text{fluid}) + bM\,(\text{solid}) \rightarrow \text{products}. \quad (1)$$

If the reaction rate of the particle is controlled by diffusion of the fluid N through the ash layer, the time t required for a spherical solid to react can be calculated by the following equation:

$$1 - 3(1-x)^{2/3} + 2(1-x) = \frac{6bDC_\circ}{C_B r_\circ^2} t = K_1 t, \quad (2)$$

where X is the uranium or iron fraction dissolved, t is the dissolution time (min), D is the diffusivity of uranium or iron ions through the ash layer (m^2/s), $C_\circ$ is the concentration of the fluid outside the particle (mol/L), C_B is the apparent concentration of the solid reactant (mol/L), $r_\circ$ is the initial outside radius of the particle (m), and K_1 and K_2 are the apparent rate constants.

If the reaction rate is controlled by chemical reaction, the integrated rate equation is expressed by the following equation:

$$1 - (1-x)^{1/3} = \frac{bk_d C_\circ}{C_B r_\circ} t = K_2 t, \quad (3)$$

where K_d is the chemical reaction rate constants. To explore the effect of temp., particle size, S/L ratio, H_2SO_4 conc. and stirring speed on the reaction kinetics of uranium and iron, a plot of $1-(1-x)1/3$ against dissolution time at different dissolution parameters is established and shown in Figs. 7, 8.

From the two shrinking core models examined, only Eq. (3) has been found to give a perfect straight line with a good correlation coefficient. Hence, all resulted data were found to fit the shrinking core model with chemical reaction model as the rate determining step.

The apparent rate constants K_1 and K_2 of uranium and iron for the two shrinking core models examined at different temperature were calculated from the slopes of the straight lines obtained from Figs. 7, 8. The values of K_1 and K_2 and their corresponding correlation coefficients are summarized in both Tables 2, 3.

The apparent rate constant values of K_2 were used to obtain the activation energy of the dissolution reaction (E_a) from the Arrhenius equation:

$$\ln K = \frac{-E_a}{R}\left(\frac{1}{T}\right) + \ln A, \quad (4)$$

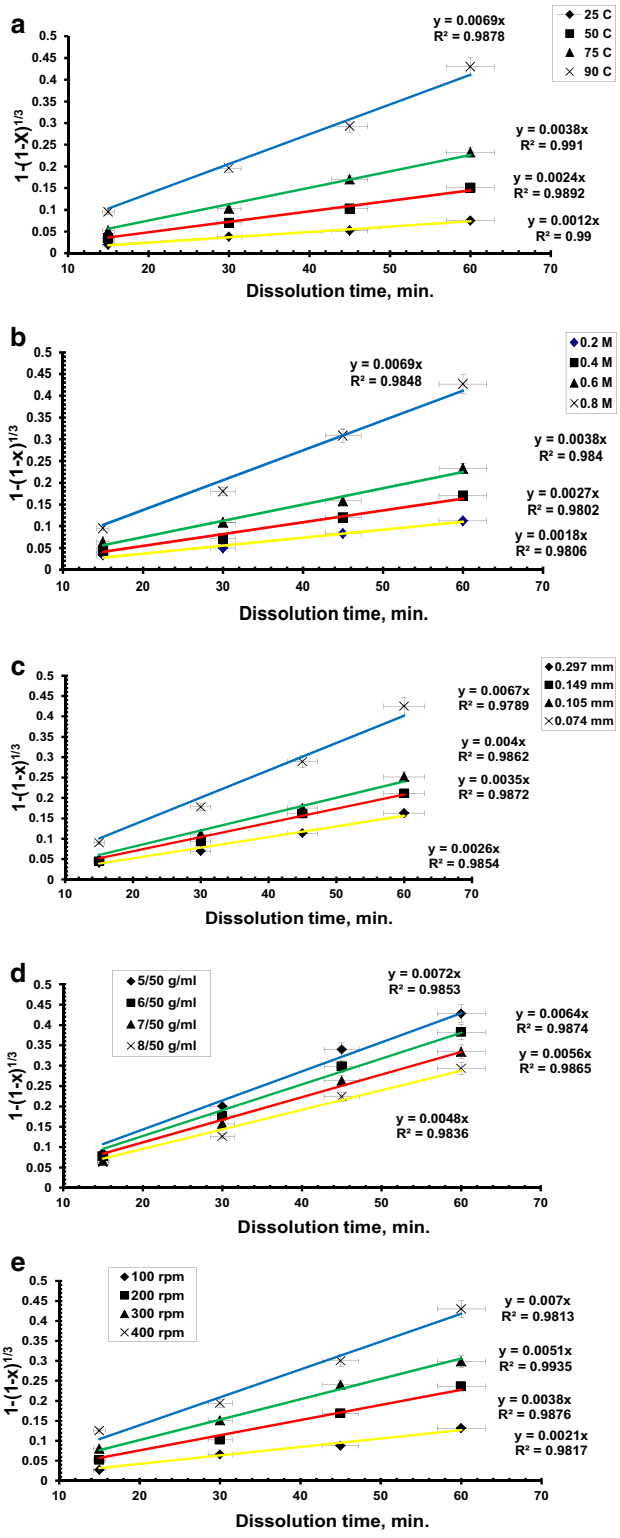

Fig. 7 Plot of $1-(1-x)^{1/3}$ against dissolution time at different parameter for uranium: **a** temperature; **b** H_2SO_4 concentration; **c** particle diameter; **d** S/L ratio; **e** stirring speed

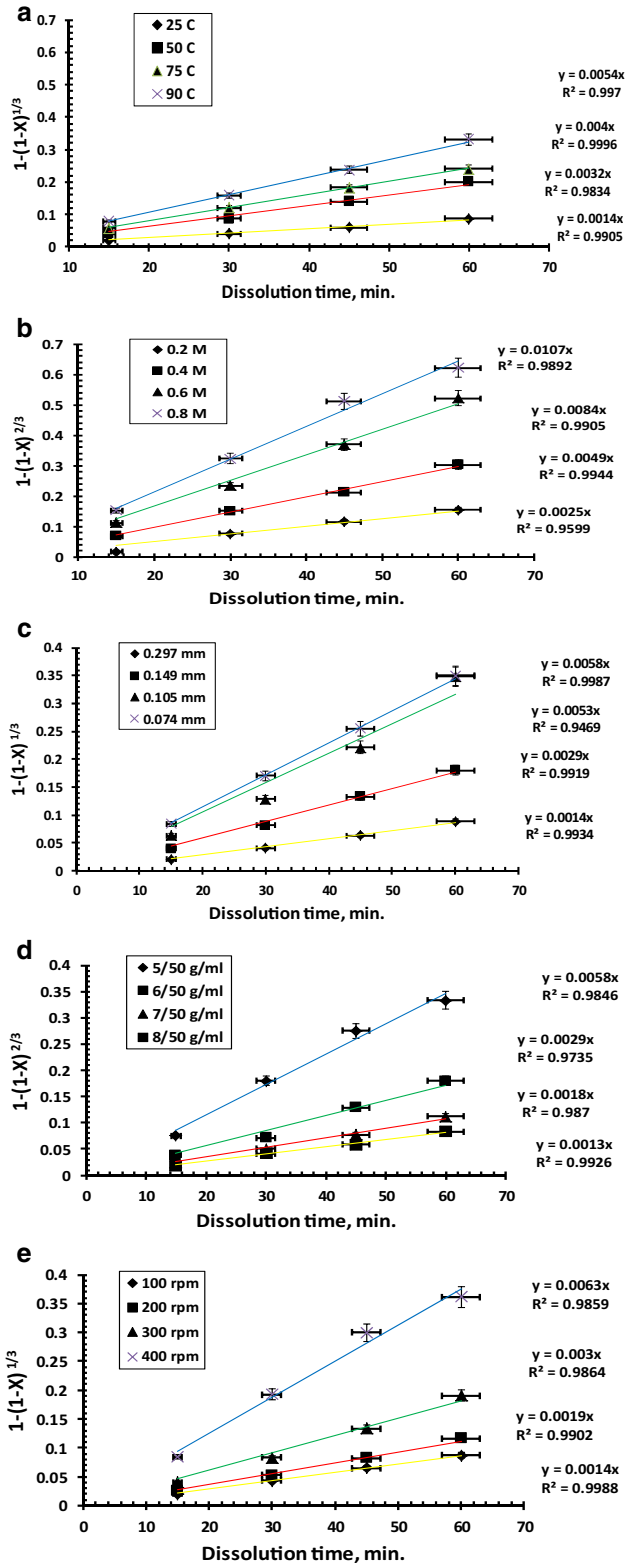

Fig. 8 Plot of $11 - (1 - x)^{1/3}$ against dissolution time at different parameter for iron: **a** temperature; **b** H_2SO_4 concentration; **c** particle diameter; **d** *S*/*L* ratio; **e** stirring speed

Table 2 Apparent rate constants (K_1, K_2) and their correlation coefficients for uranium dissolution

Temperature, °C	Apparent rate constants		Correlation coefficients (R^2)	
	K_1 (min^{-1})	K_2 (min^{-1})	R_1^2	R_2^2
25	0.0002	0.0012	0.825	0.99
50	0.0008	0.0024	0.7628	0.9892
75	0.0019	0.0038	0.7914	0.991
90	0.0043	0.0069	0.7301	0.9878

Table 3 Apparent rate constants (K_1, K_2) and their correlation coefficients for iron dissolution

Temperature, °C	Apparent rate constants		Correlation coefficients (R^2)	
	K_1 (min^{-1})	K_2 (min^{-1})	R_1^2	R_2^2
25	0.0003	0.0014	0.8104	0.9905
50	0.0014	0.0032	0.79	0.9834
75	0.003	0.004	0.7835	0.9996
90	0.0091	0.0054	0.6583	0.997

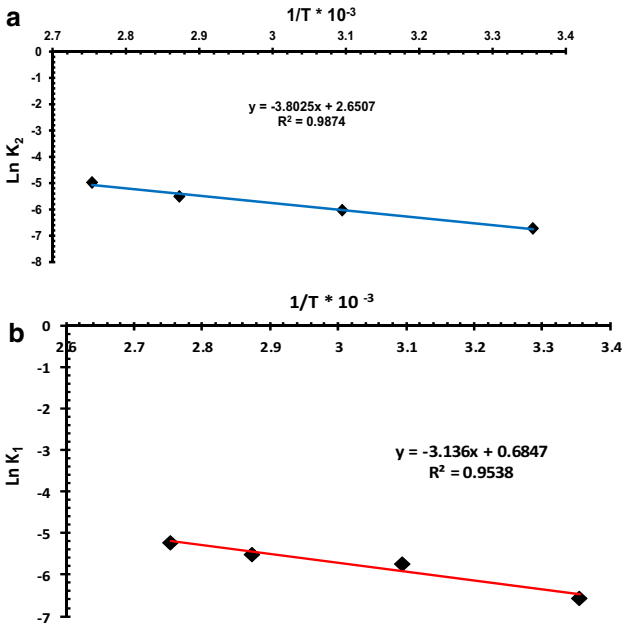

Fig. 9 Arrhenius plot of **a** uranium and **b** iron kinetic analysis

where K is the apparent rate constant, E_a is the activation energy in kJ/mol, R is the molar gas constant in J/mol K and A is the Arrhenius constant. The plot of ln K against $1/T$ in Fig. 9a, b gives a slope that represents the activation energies 31.59 kJ/mol for uranium and 26.02 kJ/mol for

iron. Hence, all resulted data are found to fit the shrinking core model with chemical reaction as a rate determining step (Yuan 2018; Luo et al. 2010; Li et al. 2011; Ekinci et al. 1998; Tavakoli et al. 2017). Also, shrinking core model (SCM) with a mixed chemical and diffusion control mechanisms was suggested in the dissolution kinetics of many ores (Souza et al. 2007; Silva 2004).

Conclusions

Based on results of mineralogical, dissolution, kinetic and thermodynamic investigations, it can be concluded that both H_2SO_4 and temperature have a significant effect on increasing uranium–iron dissolution from ferruginous siltstone ore. The dissolution rate also increases by increasing stirring speed and decreases by both particle diameter and *S*/*L* phase ratio. With 0.8 M H_2SO_4 and temperature of 90 °C using 0.075 mm particle diameter with 400 rpm, about 81.92% of uranium and 96.96% of iron are dissolved.

Studying the dissolution kinetics for both uranium and iron is very important as the two elements can be separated from each other if there is a great difference in the dissolution rate and activation energy. The dissolution kinetics and thermodynamics indicate that shrinking core model is applicable. The reaction mechanism for uranium and iron dissolution is based on chemical reaction as a rate determining step with activation energy of 31.59 kJ/mol and 26.02 kJ/mol for uranium and iron, respectively.

Therefore, I give an important information through the dissolution kinetic studies to the decision-makers in the Nuclear Materials Authority in Egypt to decide how to deal with this ore in the case of the use of sulfuric acid as a leaching agent which proved to be non-selective and that the activation energy needed to dissolve uranium and iron close together. Some will thus find the two elements with each other. Therefore, either the search for a selective leaching agent to separate uranium from iron or the design of selective extraction units to separate the two elements using different separation techniques were taken into consideration according to economic feasibility calculations.

Acknowledgements I would like to thank Nuclear Materials Authority for provision of the sample and tools necessary for the study, co-authors in particular Assistant Professor. Mohamed Farid Cheira, for following up on the work process and continuous encouragement.

Compliance with ethical standards

Conflict of interest The corresponding Author, Bahig M. Atia, and Co-authors, Mohamed A. Gado and Mohamed F. Cheira, declare that they have no conflict of interest.

References

Aday B, Pamuk H, Kaya M, Sen F (2016) Graphene oxide as highly effective and readily recyclable catalyst using for the one-pot synthesis of 1,8-dioxoacridine derivatives. J Nanosci Nanotechnol 16(6):6498–6504. https://doi.org/10.1166/jnn.2016.12432

Amme M, Svedkauskaite J, Murray M, Merino J (2007) A kinetic study of UO_2 dissolution and H_2O_2 stability in the presence of ground water ions. Radiochim Acta 95:683–692. https://doi.org/10.1524/ract.2007.95.12.683

Ayanda OS, Adekola FA (2012) Leaching of a Nigerian columbite in hydrochloric acid: dissolution kinetics. Int J Metall Eng 1(3):35–39. https://doi.org/10.5923/j.ijmee.20120103.01

Azimi A, Azari A (2017) Removal of heavy metals from industrial waste waters: a review. ChemBioEngRev 4(1):37–59. https://doi.org/10.1002/cben.201600010

Benedik L, Pintar H, Byrne AR (1999) The leachability of some natural and man-made radionuclide from soil and sediments on acid attack. Radioanal Nucl Chem 240:859–865. https://doi.org/10.1007/BF02349863

Billard I, Gaillard C, Kennig C (2007) Dissolution of UO_2, UO_3 and lanthanide oxides in BumimTf2N: effect of acid and water and formation of $UO_2(NO_3)_3^-$. Dalton Trans 8:4214–4221. https://doi.org/10.1039/b706355e

Cheira MF, El-Didamony AM, Mahmoud KF, Atia BM (2014) Equilibrium and kinetic characteristics of uranium recovery by the strong base Ambersep 920U Cl resin. IOSR-JAC 7:32–40. https://doi.org/10.9790/5736-07533240

Chung DY, Seo HS, Leo JW, Yang HB, Lee EH, Kim KW (2010) Oxidative leaching of uranium from SIMFUEL using Na_2CO_3–H_2O_2 solution. Radioanal Nucl Chem 284:123–129. https://doi.org/10.1007/s10967-009-0443-6

Dasdelen Z, Yildiz Y, Eris S, Sen F (2017) Enhanced electrocatalytic activity and durability of Pt nanoparticles decorated on GO-PVP hybride material for methanol oxidation reaction. Appl Catal B 219:511–516. https://doi.org/10.1016/j.apcatb.2017.08.014

Devasia P, Natarajan KA (2004) Bacterial leaching: biotechnology in the mining industry. Resonance 2:27–34. https://doi.org/10.1007/BF02837575

Ekinci Z, Colak S, Cakici A, Sarac H (1998) Leaching kinetics of sphalerite with pyrite in chlorine saturated water. Miner Eng 11:279–283. https://doi.org/10.1016/S0892-6875(98)00006-5

Eligwe CA, Torma AE, Devries FW (1982) Leaching of uranium ores with the H_2O_2–Na_2SO_4–H_2SO_4 system. Hydrometallurgy 9:83–95. https://doi.org/10.1016/0304-386X(82)90055-X

El-Nadi YA, Daoud JA, Ali HF (2005) Modified leaching and extraction of uranium from hydrous oxide cake of Egyptian monazite. Int J Miner Process 76:101–110. https://doi.org/10.1016/j.minpro.2004.12.005

Erken E, Esirden I, Kaya M, Sen F (2015) A rapid and novel method for the synthesis of 5-substituted 1H-tetrazole catalyzed by exceptional reusable monodisperse Pt NPs@ AC under the microwave irradiation. RSC Adv 5(84):68558–68564. https://doi.org/10.1039/c5ra11426h

Erken E, Yildiz Y, Kilbas B, Sen F (2016) Synthesis and characterization of nearly monodisperse Pt nanoparticles for C1 to C3 alcohol oxidation and dehydrogenation of dimethylamine-borane (DMAB). J Nanosci Nanotechnol 16(6):5944–5950. https://doi.org/10.1166/jnn.2016.11683

Eyal Y, Olander DR (1990a) Leaching of uranium and thorium from monazite: I. Initial leaching. Geochim Cosmochim Acta. 54:1867–1877. https://doi.org/10.1016/0016-7037(90)90257-L

Eyal Y, Olander DR (1990b) Leaching of uranium and thorium from monazite: II. Elemental leaching. Geochim Cosmochim Acta 54:1879–1887. https://doi.org/10.1016/0016-7037(90)90258-M

Eyal Y, Olander DR (1990c) Leaching of uranium and thorium from monazite: III. Leaching of radiogenic daughters. Geochim Cosmochim Acta 54:1889–1896. https://doi.org/10.1016/0016-7037(90)90259-N

Fouad HK (2010) Determination of hexavalent and tetravalent uranium in phosphate ores through hydrochloric acid selective leaching. Radioanal Nucl Chem 285:193–197. https://doi.org/10.1007/s10967-010-0540-6

Gado MA (2018) Sorption of thorium using magnetic graphene oxide polypyrrole composite synthesized from natural source. Sep Sci Technol 53(13):2016–2033. https://doi.org/10.1080/01496395.2018.1443130

Goff GS, Brondax LF, Cisneros MR, Peper SM, Field SE, Scott BL, Runde WH (2008) First identification and thermodynamic characterization of ternary U (VI) species $UO_2(O_2)(CO_3)_2^{4-}$ in UO_2–H_2O_2–K_2CO_3 solutions. Inorg Chem 47:1984–1990. https://doi.org/10.1021/ic701775g

Haque KE, Laliberte JJ (1987) Batch and counter-current acid leaching of uranium ores. Hydrometallurgy 17:229–238. https://doi.org/10.1016/0304-386X(87)90054-5

Ibrahim HA, El-Sheikh EM (2011) Bioleaching treatment of Abu Zeneima uraniferrous gibbsite ore material for recovering U, REES, Al and Zn. Res J Chem Sci 1(4):55–66 **(ISSN 2231-606X)**

International Atomic Energy Agency (1990) Manual on laboratory testing for uranium ore processing. Technical report series no. 313. IAEA, Vienna, pp 35–46

Janberty L, Dorgat N, Decossas J, Delpech V, Gloaguen V, Sol V (2013) Optimization of the arsenazo-III method for the determination of uranium in water and plant samples. Talanta 115:751–754. https://doi.org/10.1016/j.talanta.2013.06.046

Karatepo O, Yildis Y, Pamuk H, Eris S, Dasdelen Z, Sen F (2016) Enhanced electrocatalytic activity and durability of highly monodisperse Pt@PPy–PANI nanocomposites as a novel catalyst for the electro-oxidation of methanol. RSC Adv 6:50851–50857. https://doi.org/10.1039/c6ra06210e

Ketzinel Z, Volkman Y, Hassid M, Azaria M (1984) On the possibility of high temperature selective leaching of uranium from raw phosphorites. Hydrometallurgy 12:129–132. https://doi.org/10.1016/0304-386X(84)90053-7

Khawassek YM, Eliwa AA, Haggag EA, Mohamed SA, Omar SA (2016a) Kinetics leaching process of uranium ions from El-Erediya rock by sulfuric acid solution. Int J Nucl Energy Sci Eng 6:35–48. https://doi.org/10.14355/ijnese.2016.06.004

Khawassek YM, Taha MH, Eliwa AA (2016b) Kinetics of leaching process using sulfuric acid for sella uranium ore material, South Eastern Desert, Egypt. Int J Nucl Energy Sci Eng 6:62–73. https://doi.org/10.14355/ijnese.2016.06.006

Lee EH, Lim JM, Chung DY, Yang HB, Yoo JH, Kim KW (2009) The oxidative dissolution behavior of fission products in a Na_2CO_3–H_2O_2 solution. Radioanal Nucl Chem 281:339–346. https://doi.org/10.1007/s10967-009-0018-6

Li G, Rao M, Jiang T, Huang Q, Peng Z (2011) Leaching of limonitic laterite ore by acidic thiosulfate solution. Miner Eng 24:859–863. https://doi.org/10.1016/j.mineng.2011.03.010

Luo W, Feng Q, Ou L, Zhang G, Chen Y (2010) Kinetics of saprolitic laterite leaching by sulfuric acid at atmospheric pressure. Miner Eng 23:458–462. https://doi.org/10.1016/j.mineng.2009.10.006

Mathew KJ, Mason B, Morales ME, Narayann UI (2009) Uranium assay determination using Davies and Gray titration: an overview and implementation of GUM uncertainty evaluation. Radioanal Nucl Chem 282:939–944. https://doi.org/10.1007/s10967-009-0186-4

Peper SM, Brondax LF, Field SE, Zehnder RA, Valdez SN, Runde WH (2004) Kinetic study of the oxidative dissolution of UO_2 in aqueous carbonate media. Ind Eng Chem Res 43:8188–8193. https://doi.org/10.1021/ie049457y

Pulhani VA, Dafauti S, Hegde AG (2007) Leaching of uranium, radium and thorium from vertisol soil by ground water. Radioanal Nucl Chem 274(2):341–343. https://doi.org/10.1007/s10967-007-1120-2

Schimmack W, Gerstmann U, Schultz OW (2005) Leaching of depleted uranium in soil as determined by column-experiments. Radiat Environ Biophys 44:183–191. https://doi.org/10.1007/s00411-005-0013-4

Sen B, Kuzu S, Demir E, Akocak S, Sen F (2017a) Highly monodisperse RuCo nanoparticles decorated on functionalized multiwalled carbon nanotube with the highest observed catalytic activity in the dehydrogenation of dimethylamine–borane. Int J Hydrog Energy 42(36):23292–23298. https://doi.org/10.1016/j.ijhydene.2017.06.032

Sen B, Kuzu S, Demir E, Akocak S, Sen F (2017b) Monodisperse palladium–nickel alloy nanoparticles assembled on graphene oxide with the high catalytic activity and reusability in the dehydrogenation of dimethylamine–borane. Int J Hydrog Energy 42(36):23276–23283. https://doi.org/10.1016/j.ijhydene.2017.05.113

Sen B, Kuzu S, Demir E, Akocak S, Sen F (2017c) Polymer-graphene hybride decorated Pt nanoparticles as highly efficient and reusable catalyst for the dehydrogenation of dimethylamine–borane at room temperature. Int J Hydrog Energy 42(36):23284–23291. https://doi.org/10.1016/j.ijhydene.2017.05.112

Sen B, Kuzu S, Demir E, Okyay TO, Sen F (2017d) Hydrogen liberation from the dehydrocoupling of dimethylamine–borane at room temperature using novel and highly monodispersed RuPtNi nanocatalysts decorated with graphene oxide. Int J Hydrog Energy 42(36):23299–23306. https://doi.org/10.1016/j.ijhydene.2017.04.213

Shakir K, Aziz M, Beheir SG (1992a) Studies on uranium recovery from a uranium bearing phosphatic sandstone by a combined heap leaching-liquid gel extraction process 1: heap leaching. Hydrometallurgy 31:29–40. https://doi.org/10.1016/0304-386X(92)90106-A

Shakir K, Aziz M, Beheir SG (1992b) Studies on uranium recovery from a uranium bearing phosphatic sandstone by a combined heap leaching-liquid gel extraction process 2: heap leaching. Hydrometallurgy 31:41–54. https://doi.org/10.1016/0304-386X(92)90107-B

Sharma JN, Bhattacharya K, Swami RG, Tangri SK, Mukherjee TK (1996) Studies on the kinetics of UO_2 dissolution in carbonate-bicarbonate medium using sodium hypochlorite as oxidant. Radioanal Nucl Chem 214:223–233. https://doi.org/10.1007/BF02163251

Silva GA (2004) Relative importance of diffusion and reaction control during the bacterial and ferric sulphate leaching of zinc sulphide. Hydrometallurgy 73:313–324. https://doi.org/10.1016/j.hydromet.2003.12.004

Singh G, Singhal RK, Malav RK, Fulzele A, Prakash A, Afzal M, Panakkal JP (2011) A comparative study on dissolution rate of sintered (Th–U)O_2 pellets in nitric acid by microwave and conventional heating. Anal Methods 3:622–627. https://doi.org/10.1039/C0AY00630K

Smirov AL, Rychkov VN, Umanskii AB, Galyanina EA, Klyusnikov AM (2009) Kinetic features of underground uranium leaching from ores of hydrogenous uranium deposits. Radiochemistry 51:61–64. https://doi.org/10.1134/S1066362209010147

Souza AD, Pina PS, Leo VA, Silva CA, Siqueira PF (2007) The leaching kinetics of zinc sulphide concentrate in acid ferric sulphate. Hydrometallurgy 89:72–81. https://doi.org/10.1016/j.hydromet.2007.05.008

Tavakoli HZ, Abdollahy M, Ahmadi SJ, Darban AK (2017) Kinetics of uranium bioleaching in stirred and column reactor. Miner Eng 111:36–46. https://doi.org/10.1016/j.mineng.2017.06.003

Umanskii AB, Klyushnikov AM (2011) Development of SO_2/O_2 system as an oxidant at uranium leaching processes. Radioanal Nucl Chem 292:885–888. https://doi.org/10.1007/s10967-011-1572-2

Volkovich VA, Griffiths TR, Fray DJ, Thied RC (2000) A new method for determining oxygen solubility in molten carbonates and carbonate–chloride mixtures using the oxidation of UO_2 to uranate reaction. J Nucl Mater 282:152–158. https://doi.org/10.1016/S0022-3115(00)00427-X

Wei L, Mo-tang T, Chao-bo T, Jing H, Sheng-hai Y, Jian-guang Y (2010) Dissolution kinetics of low grade low complex copper ore in ammonia-ammonium chloride solution. Trans Nonferrous Metals Soc 20:910–917. https://doi.org/10.1016/S1003-6326(09)60235-1

Yao IA, Chu T (2013) Fe-containing ionic liquids as effective and recoverable oxidants for dissolution of UO_2 in the presence of imidazolium chlorides. Dalton Trans 42:8413–8419. https://doi.org/10.1039/C3DT32832E

Yildiz Y, Erken E, Pamuk H, Sert H (2016) Monodisperse Pt nanoparticles assembled on reduced graphene oxide: highly efficient and reusable catalyst for methanol oxidation and dehydrocoupling of dimethylamine-borane (DMAB). J Nanosci Nanotechnol 16(6):5951–5958. https://doi.org/10.1166/jnn.2016.11710

Yildiz Y, Kuzu S, Sen B, Savk A, Akocak S, Sen F (2017a) Different ligand based monodispersed Pt nanoparticles decorated with rGO as highly active and reusable catalysts for the methanol oxidation. Int J Hydrog Energy 42(18):13061–13069. https://doi.org/10.1016/j.ijhydene.2017.03.230

Yildiz Y, Okyay TO, Sen B, Gezer B, Kuzu S, Savk A, Demir E, Dasdelen Z, Sert H, Sen F (2017b) Highly monodisperse Pt/Rh nanoparticles confined in the graphene oxide for highly efficient and reusable sorbents for methylene blue removal from aqueous solutions. ChemistrySelect 7:697–701. https://doi.org/10.1002/slct.201601608

Yuan F (2018) Study on kinetics of Fe (II) oxidized by air in $FeSO_4$–H_2SO_4 solutions. Miner Eng 121:164–168. https://doi.org/10.1016/j.mineng.2018.03.013